Supplementary Materials

Materials and Methods

Animals. 8-to-12-week-old mice, fed *ad libitum* and housed at 22ºC under 12 hour light:dark cycle were used in these experiments. *Arntl*$^{LoxP/LoxP}$ mice on C57BL6/J background (*B6.129S4(Cg)-Arntl*^{tm1Weit}*/J*) were backcrossed for 10 generations onto C57BL/6J (*Nnt*$^{-/-}$) background, and then subsequently crossed with *Lyz2*^{Cre} mice (*B6.129P2-Lyz2*$^{tm1(cre)Ifo}$*/J*) to generate *Arntl*$^{LoxP/LoxP}$*Lyz2*^{Cre} mice. *Ccr2*$^{-/-}$ mice on the C57BL/6J background were obtained from the Charo laboratory.

Monocyte isolation and macrophage culture. Blood monocytes and peritoneal macrophages were isolated using magnetic microbeads (Miltenyi) coupled to anti-CD115 antibody (clone AFS98, Biolegend). Prior to magnetic isolation, each blood sample (pooled from 5 mice) was centrifuged over a Ficoll gradient to remove granulocytes and RBCs. The purity of isolated cells was confirmed by flow cytometry and was routinely >95%. To activate circadian cycling in cultured cells, bone marrow-derived macrophages (BMDMs) were stimulated with 50% horse serum for 2 hours, as described previously (*38*). Subsequently, synchronized BMDMs were harvested at the indicated intervals for gene expression and immunoprecipitation studies.

Flow cytometry and ELISAs. Blood samples were subjected to RBC lysis, and spleens were homogenized and filtered through a 40 μm strainer (BD) to remove large cellular debris. eWAT and BAT were homogenized and digested with Collagenase I (2 mgml^{-1}, Worthington) for 20 minutes at 37°C in a shaker (250 rpm). The digested cell suspensions were passed through a 40 μm strainer, and subjected to centrifugation to separate the stromal vascular cells from adipocytes. Pelleted cells were re-suspended in

FACS buffer (PBS, 5% FBS, 5 mM EDTA) for antibody staining and analyses. The following antibodies directed against mouse antigens were used: CD3 (clone 145-2C11), CD4 (clone GK1.5), CD8 (clone 53-6.7), B220 (clone RA3-6B2), Ly6C (clone HK1.4), Ly6G (clone 1A8), CD11b (clone M1/70), CD11c (clone N418), CD45 (clone 30-F11), CD49b (clone DX5), CD115 (clone AFS98), F4/80 (clone BM8), TNFα (clone MP6-XT22), and IFNγ (clone XMG1.2, all from Biolegend); Siglec-F (clone E50-2440) and CCL2 (clone 2H5, BD Biosciences); FcεR1 (clone MAR-1, eBioscience); CCL8 (bs1985R) and S100A8 (bs2696R, Bioss); CD301 (clone ER-MP23, AbdSerotec); iNOS (sc-7271, Santa Cruz); anti-rabbit (A21246) and anti-mouse IgG (A21235, Invitrogen). Samples were fixed (FACS buffer plus 1% paraformaldehyde) and stored at 4ºC prior to analysis. Data was acquired on FACSVerse (BD) and analyzed using FlowJo (Treestar). Inflammatory cytokines (IL1β, IL6, IL12, TNFα, and IFNγ) and chemokines (CCL2 and CCL8) in serum samples, peritoneal fluid, and culture media were detected by cytometric bead arrays (BD) and ELISAs (R&D), as per manufacturers' protocol. Cytokine and chemokine concentration in peritoneal fluid was normalized to total protein.

Thioglycollate elicitation. Mice were intraperitoneally injected with 2 ml of thioglycollate broth (BD), and the peritoneal cavity was flushed with 5 ml of PBS 30 mins or 2 hours later. Cells were pelleted for flow cytometric analysis, and the supernatants were analyzed for cytokine and chemokines.

***Listeria* infection.** *L. monocytogenes* 10403S expressing green fluorescent protein (DH-L1252) was grown to mid-log (OD_{600} 0.25-0.5) in brain-heart infusion (BHI) medium (Difco) (*39*). Adult male and female mice were infected with *L. monocytogenes* via intraperitoneal injection with the stated number of bacteria. Serial dilutions of all inocula

were plated onto BHI agar plates for enumeration. At intervals following infection, peritoneal fluid, liver, and spleen were homogenized for colony forming unit (CFU) determination.

Immunoprecipitation. Chromatin immunoprecipitations were performed using serum shocked BMDMs, and antibodies against BMAL1 (ab3350) and CLOCK (ab3517, Abcam); EZH2 (clone D2C9), tri-methylated H3K4 (clone C42D8), tri-methylated H3K27 (clone C36B11), and Rbp1 (clone 4H8, all from Cell Signaling) with chromatin immunoprecipitation assay kits (Cell Signaling). Primers used to amplify the precipitated chromatin are listed in tables S1 and S2. E-boxes were identified at positions -2428 (CATCTG for *Ccl2*); -223 and -293 (CAGATG for *Ccl8*); and -4381 (CACCTG for *S100a8*). For the co-immunoprecipitation experiments, serum shocked BMDMs (ZT8) were lyzed in 20 mM Tris-HCl, 10 mM KCl, 1 mM EDTA, 0.1% NP40, 10% Glycerol, 1:200 Protease Inhibitor Cocktail (pH 7.5), and pre-cleared with agarose beads (Cell Signaling) before immunoprecipitation with 5 μg anti-BMAL1 antibody (ab3350, Abcam) per 1 ml lysate. Immunoprecipitated proteins were analyzed using BMAL1 (ab3350), CLOCK (ab3517, Abcam); EZH2 (clone D2C9) and SUZ12 (clone D39F6, Cell Signaling); and EED antibodies (17-663, EMD Millipore).

Quantitative RT-PCR. RNA was isolated from cells or tissues using the TRIzol reagent (Invitrogen). Reverse transcription was carried out using First-strand cDNA Synthesis kit (Origene), and quantitative PCR reactions were performed on CFX384 real-time PCR detection system (Bio-Rad). Relative expression level of mRNAs was calculated using the comparative CT method using 36B4 as an internal control. Primers used for qRT-PCR analysis are listed in table S3.

Diet-induced obesity. 6-week-old male mice were fed with 60% kcal fat diet (Research Diets, D12492) to promote obesity. Body composition was assessed by DEXA, whereas Oxygen consumption, RER, and total activity were quantified using the CLAMS system (Columbus Instruments). Intraperitoneal glucose (1 gkg^{-1}) and insulin (1 Ukg^{-1}) tolerance tests were performed in overnight-fasted and 6-hour-fasted mice, respectively. For analysis of insulin signaling, mice were injected with insulin (1 Ukg^{-1}) through the inferior vena cava, and liver, eWAT, and quadriceps were isolated after 2, 5, and 7 minutes, respectively. Tissues lysates were immunoblotted for total (9272S) and phosphorylated AKT (clone 193H12, Cell Signaling). Total JNK (clone 56G8) and pJNK (9251S) were detected in total lysates using antibodies from Cell Signaling. For short term HFD feeding, mice were housed at 30ºC and fed HFD for one week. Immune cell numbers were subsequently quantified in blood and adipose tissues, as described previously (*40*). For time restricted feeding, mice were given free access to food only during the 12-hour light:dark cycle for 14 days.

Statistical analysis. All data are presented as means ± SEMs and analyzed using Prism (GraphPad). Statistical significance is determined using the two-tailed Student's t-test, one-way and two-way analysis of variance tests, and log-rank test for pair-wise comparisons, multiple-group comparisons, and survival analyses, respectively. A p-value of <0.05 was considered to be statistically significant.

Supplementary Figures

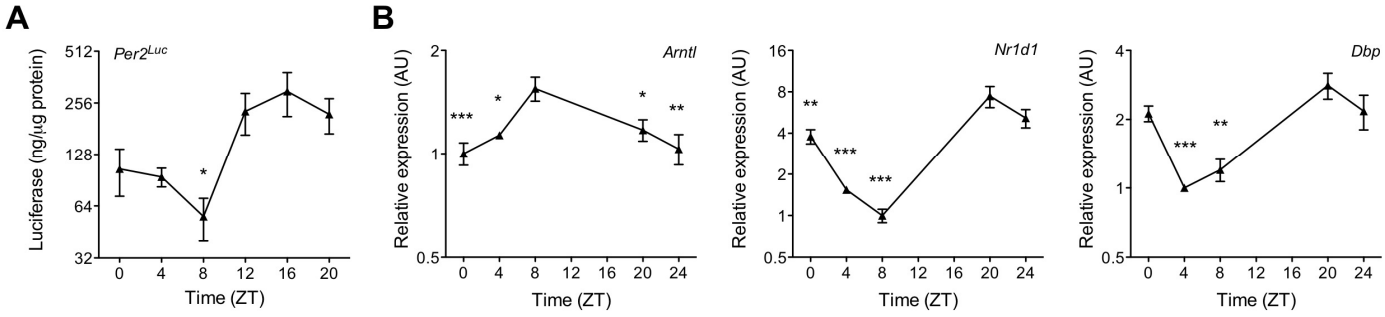

fig. S1. Diurnal variation of clock genes in monocytes. (**A**) Expression of luciferase protein in blood monocytes isolated from *Per2*^{Luc} mice (n = 3 samples per time point). (**B** to **D**) Quantitative PCR analysis of *Arntl*, *Nr1d1*, and *Dbp* mRNAs in serum-shocked THP1 over 24 hours (n = 4-5 samples per time point). Pooled data from two independent experiments are presented as mean ± SEM and statistically analyzed using two-tailed Student's t-tests (A) and one-way ANOVA (B-D) (comparisons were made between the acrophase and other time points). **P*<0.05; ***P*<0.01; ****P*<0.001.

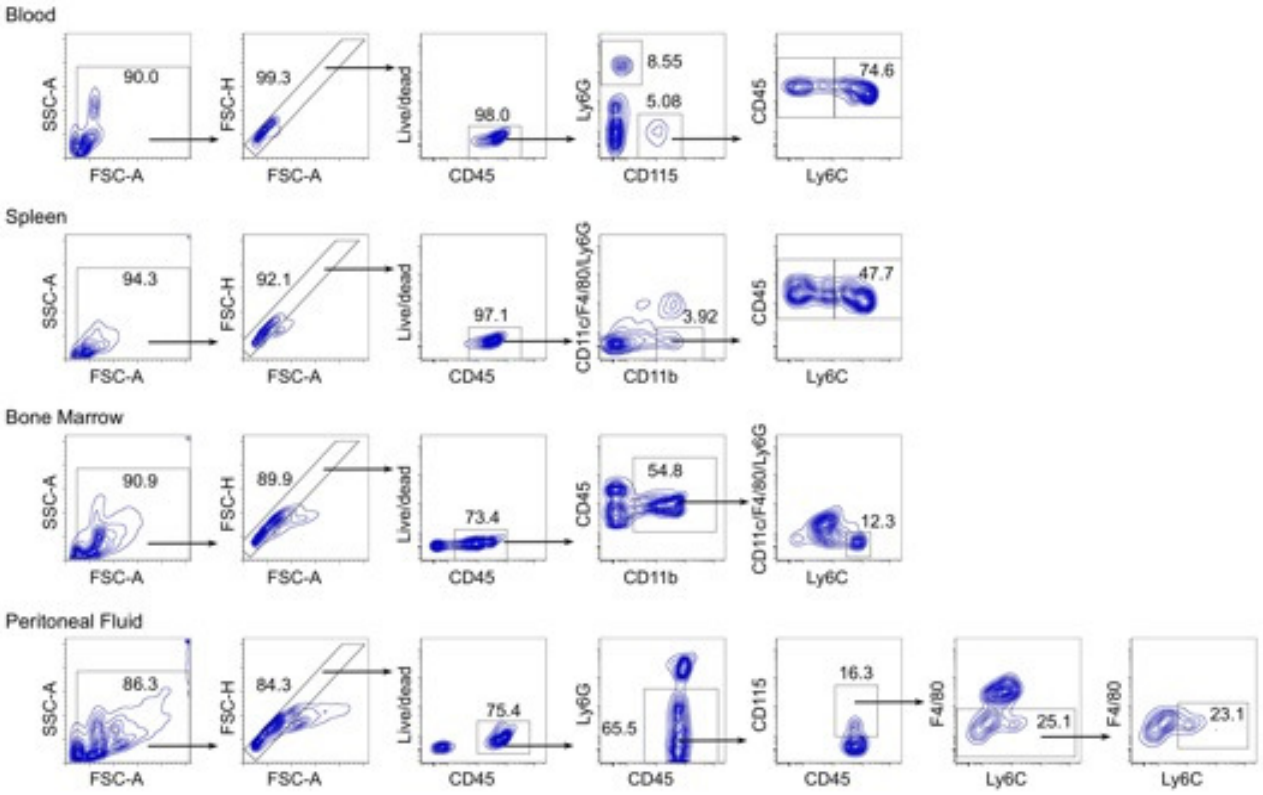

fig. S2. Gating strategy of monocytes in different tissues. Mononuclear cells from blood or tissues were gated for forward and side-scatter (FSC/SSC), doublets, and live/dead prior to identification of blood ($CD45^+CD115^+Ly6G^-$), splenic ($CD45^+CD11b^+CD11c^-F4/80^-Ly6G^-$), bone marrow ($CD45^+CD11b^+CD11c^-F4/80^-Ly6G^-Ly6C^+$), and peritoneal ($CD45^+CD115^+Ly6G^-F4/80^-$) monocytes.

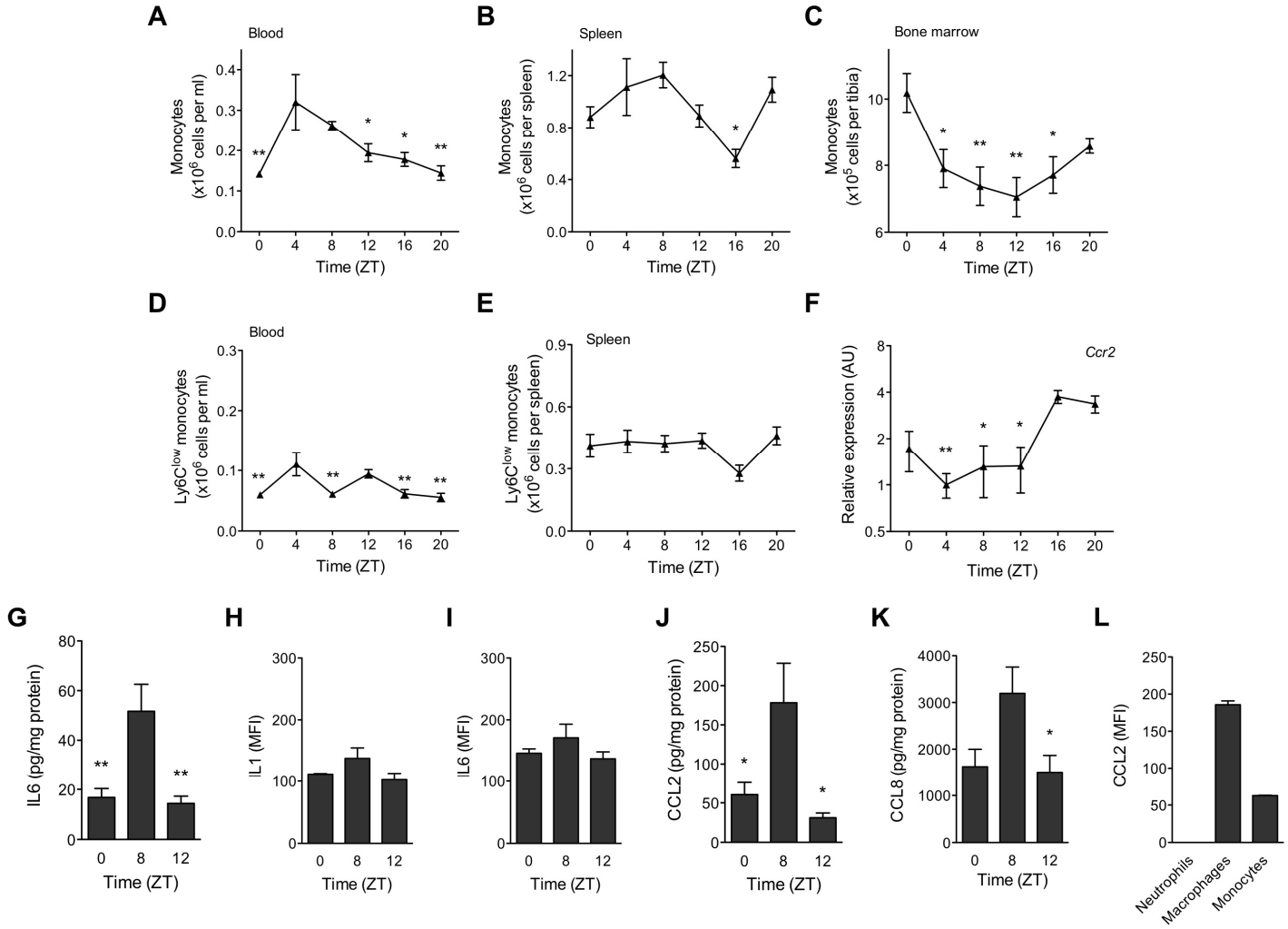

fig. S3. Diurnal variation in monocyte number and inflammation. (**A** to **C**) Total monocyte numbers in blood (A), spleen (B), and bone marrow (C) as quantified during a 12 hour light-dark cycle (n = 5 mice per time point). (**D** and **E**) Numbers of Ly6C^{low} monocytes in blood (D) and spleen (E) during a 12 hour light-dark cycle (n = 5 mice per time point). (**F**) Quantitative RT-PCR analysis of *Ccr2* mRNA expression in blood monocytes during a 12 hour light-dark cycle (n = 3-4 samples per time point). (**G** to **K**) Concentration of IL6 (G), CCL2 (J), and CCL8 (K) in the peritoneal fluid 2 hours after

elicitation with thioglycollate. Intracellular staining for IL1 (H) and IL6 (I) in Ly6C^{hi} monocytes 2 hours after elicitation with thioglycollate expression (n = 5 mice per ZT). (**L**) Intracellular staining for CCL2 in Ly6C^{hi} monocytes, macrophages, and neutrophils 30 mins after injection of thioglycollate (n = 5 mice). Representative (A to E) or pooled data (F and G, J and K) of two independent experiments are shown as mean ± S.E.M and statistically analyzed using one-way ANOVA. Comparisons were made between the acrophase and other time points $*P<0.05$; $**P<0.01$.

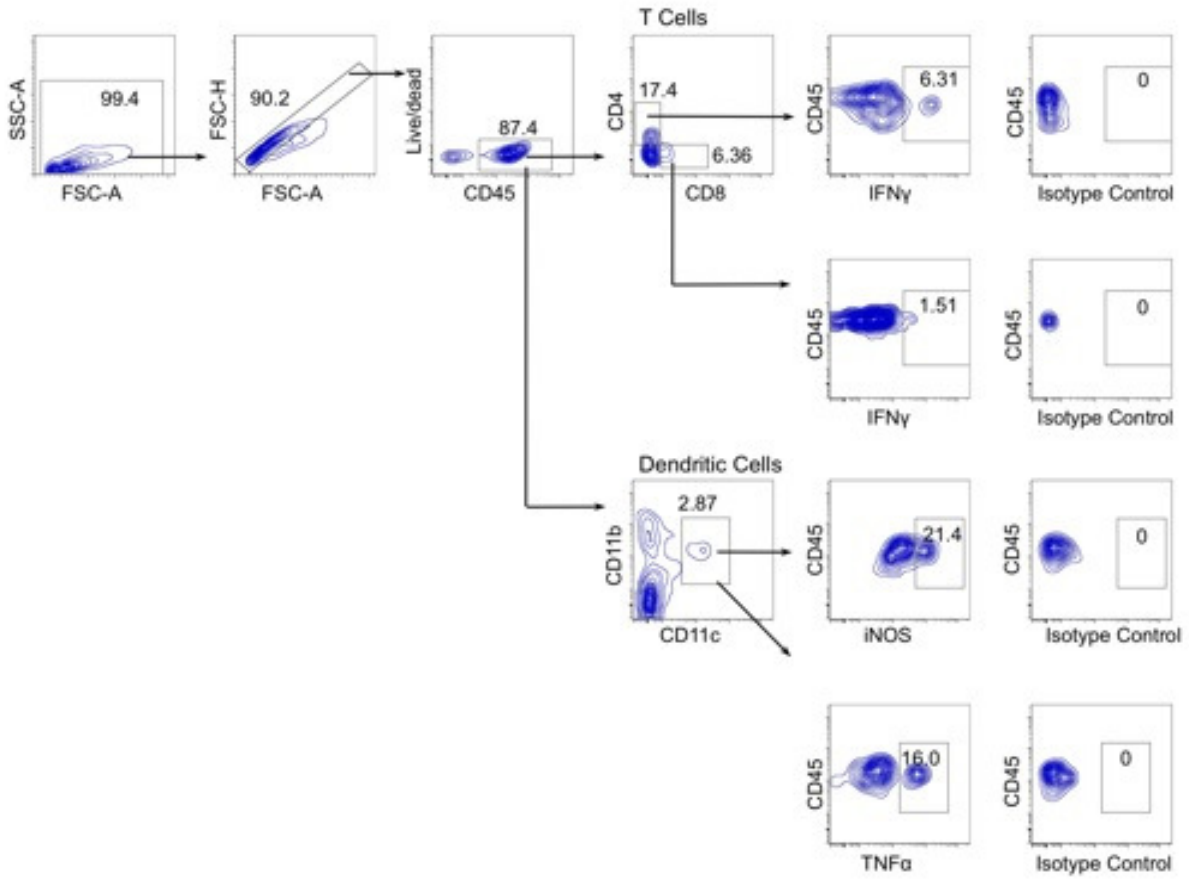

fig. S4. Gating strategy for identifying cytokine producing cells in mice infected with *L. monocytogenes*. Mononuclear cells were gated for forward and side-scatter (FSC/SSC), doublets, and live/dead prior to analysis of $CD4^{+}IFN\gamma^{+}$ T cells, $CD8^{+}IFN\gamma^{+}$ T cells, $CD11c^{+}TNF\alpha^{+}$, and $CD11c^{+}iNOS^{+}$ dendritic cells.

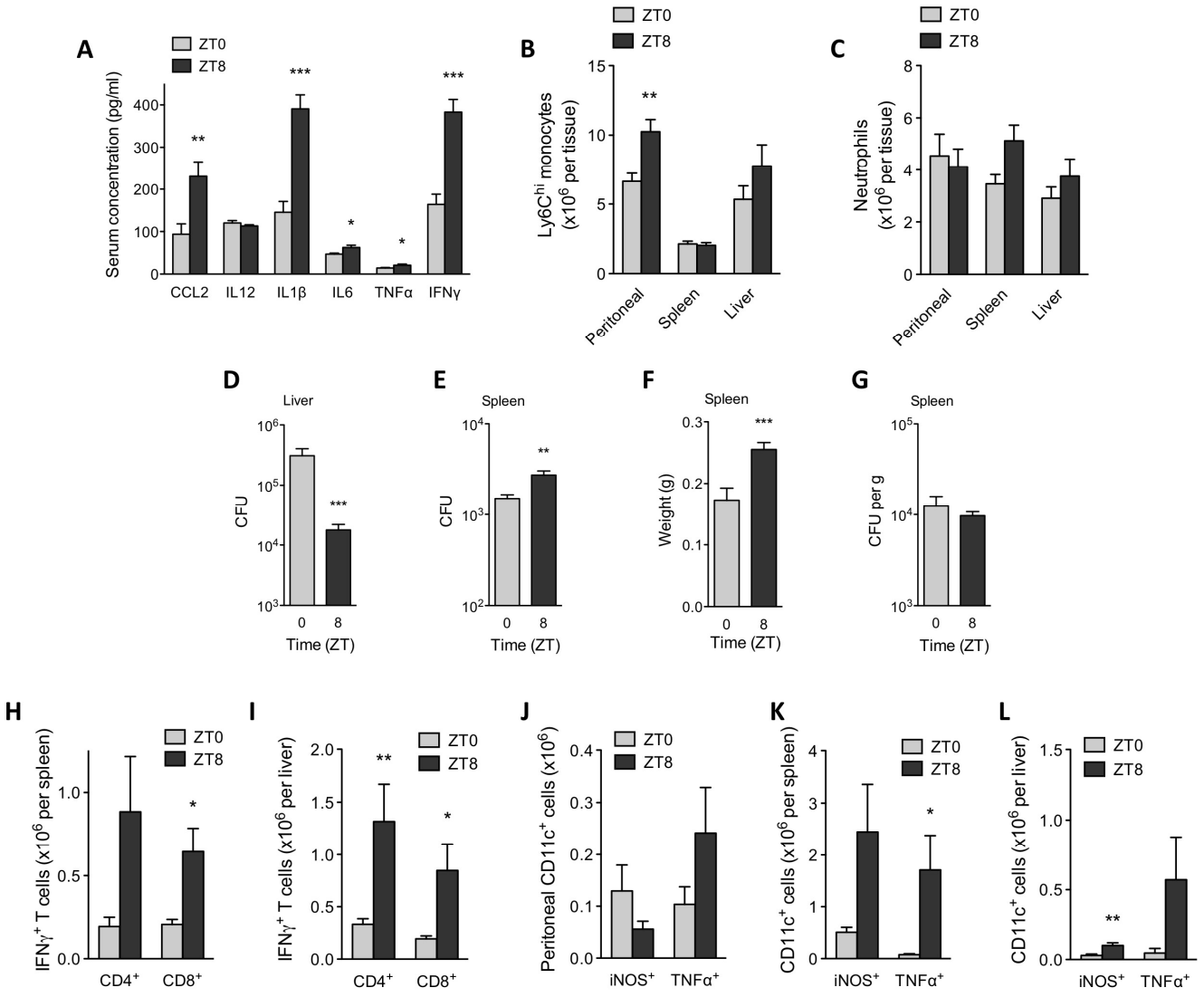

fig. S5. Diurnal variation in host response to *L. monocytogenes*. Wild type mice kept on a 12 hour light-dark cycle were intraperitoneally inoculated with $1x10^6$ *L. monocytogenes* at ZT0 and ZT8. (**A**) Concentration of chemokines and cytokines in serum 2 dpi (n = 15 mice per time point). (**B** and **C**) Numbers of $Ly6C^{hi}$ monocytes (B) and neutrophils (C) in different tissues of mice 2dpi (n=15 mice per time point). (**D** and

E) *L. monocytogenes* colony forming units (CFUs) recovered from the liver (D), and spleen (E) were quantified 6 dpi (n = 8-10 mice per time point). (**F**) Spleen weight at 6 dpi (n = 8-10 mice per time point). (**G**) CFUs normalized to spleen weight at 6 dpi (n = 8-10 mice per time point). (**H** and **I**) Numbers of IFNγ^+ CD4$^+$ and CD8$^+$ T cells in spleen (H) and liver (I) 6 dpi (n = 10-15 mice per time point). (**J** to **L**) Numbers of iNOS$^+$CD11c$^+$ and TNFα^+CD11c$^+$ cells in peritoneal cavity (J), spleen (K), and liver (L) of mice 6 dpi (n = 8-10 mice per time point). Pooled data from two to three independent experiments are shown as mean ± S.E.M. Two-tailed Student's *t*-tests are used for statistical analyses. **P*<0.05; ***P*<0.01; ****P*<0.001.

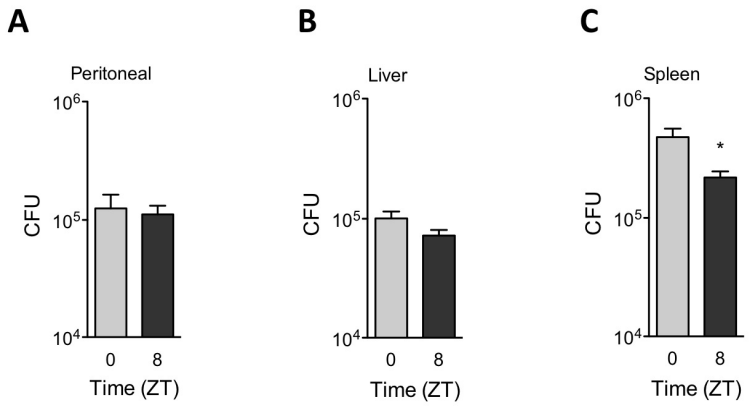

fig. S6. High dose intraperitoneal infection with *L. monocytogenes*. (**A** to **C**) Wild type mice kept on a 12 hour light-dark cycle were intraperitoneally inoculated with $1x10^7$ *L. monocytogenes* at ZT0 and ZT8, and CFUs recovered from peritoneal cavity (A), liver (B), and spleen (C) were quantified 2 dpi (n = 10 mice per time point). Pooled data from two independent experiments are shown as mean ± S.E.M and statistically analyzed using two-tailed Student's *t*-test. *$P<0.05$.

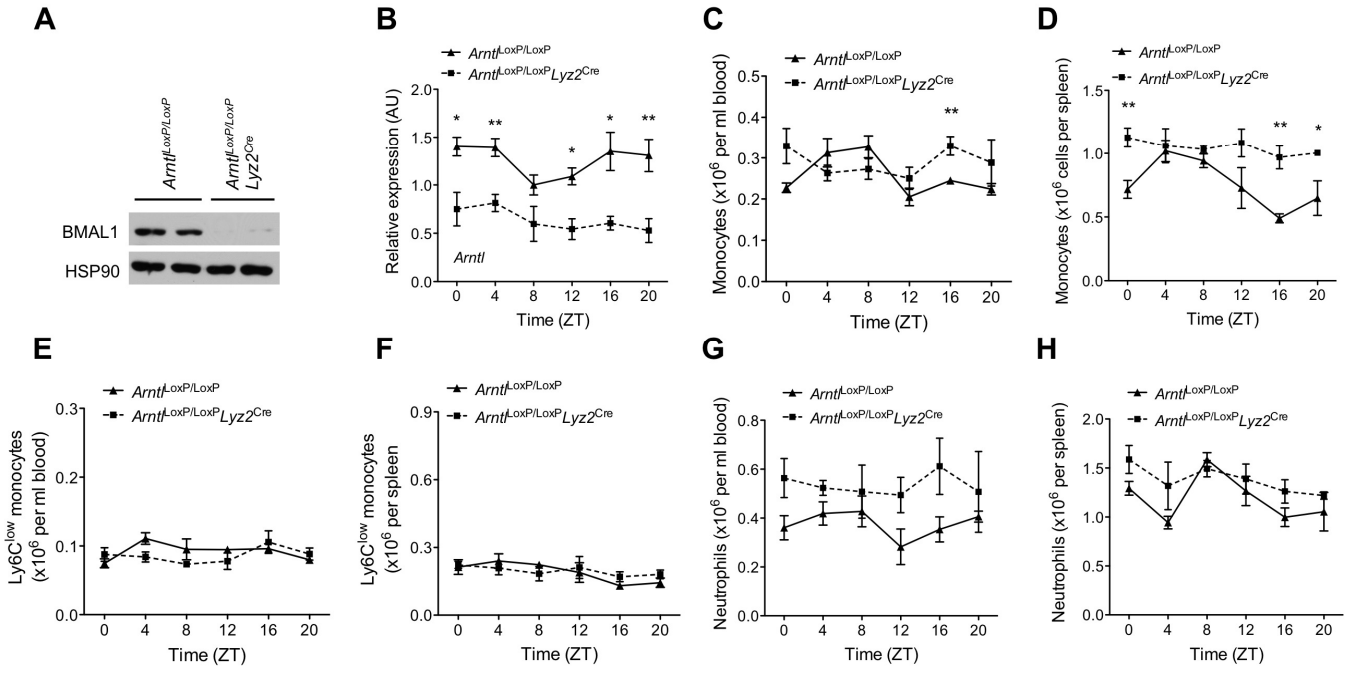

fig. S7. Deletion of *Arntl* in myeloid cells disrupts monocyte rhythms. (**A**) Immunoblot of BMAL1 protein in blood monocytes isolated from *Arntl*$^{LoxP/LoxP}$ and *Arntl*$^{LoxP/LoxP}$*Lyz2*^{Cre} mice at ZT0. (**B**) Quantitative RT-PCR analysis of *Arntl* mRNA in blood monocytes of *Arntl*$^{LoxP/LoxP}$ and *Arntl*$^{LoxP/LoxP}$*Lyz2*^{Cre} mice kept on a 12 hour light-dark cycle at the various ZTs (n = 3-4 samples per genotype and time point). (**C** and **D**) Total monocyte numbers in blood (C) and spleen (D) of *Arntl*$^{LoxP/LoxP}$ and *Arntl*$^{LoxP/LoxP}$*Lyz2*^{Cre} mice during the 12 hour light-dark cycle (n = 5 mice per genotype and time point). (**E** and **F**) Ly6C^{low} monocyte numbers in blood (E) and spleen (F) of *Arntl*$^{LoxP/LoxP}$ and *Arntl*$^{LoxP/LoxP}$*Lyz2*^{Cre} mice at various ZTs (n = 5 mice per genotype and time point). (**G** and **H**) Neutrophil numbers in blood (G) and spleen (H) of *Arntl*$^{LoxP/LoxP}$ and *Arntl*$^{LoxP/LoxP}$*Lyz2*^{Cre} mice during the 12 hour light-dark cycle (n = 5 mice per

genotype and time point). Pooled data (A and B) or representative (C to F) from two to three independent experiments are shown as mean ± S.E.M. Two-tailed Student's t-tests were used for statistical analyses. *P<0.05; **P<0.01 comparison between *Arntl*$^{LoxP/LoxP}$ and *Arntl*$^{LoxP/LoxP}$*Lyz2*^{Cre} at each time point.

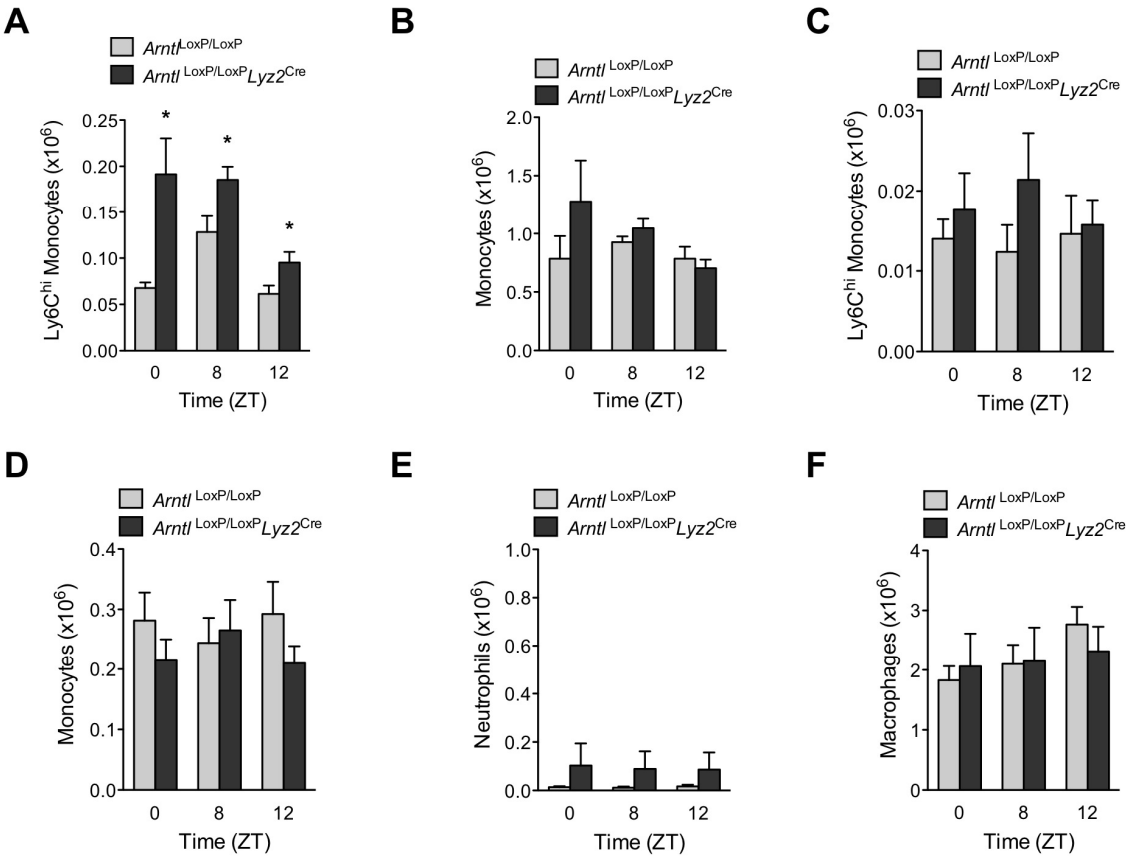

fig. S8. Loss of diurnal variation in thioglycollate-induced sterile peritonitis in *Arntl*$^{LoxP/LoxP}$*Lyz2*^{Cre} mice. (**A** and **B**) Numbers of Ly6C^{hi} (A) and total (B) monocytes in the peritoneum of *Arntl*$^{LoxP/LoxP}$ and *Arntl*$^{LoxP/LoxP}$*Lyz2*^{Cre} mice kept under a 12 hour light-dark cycle 2 hours after injection with thioglycollate at different ZTs (n = 5 mice per genotype and time point). (**C** to **F**) Resident numbers of Ly6C^{hi} (C) and total (D) monocytes, neutrophils (E), and macrophages (F) in peritoneal cavity of mice kept under a 12 hour light-dark cycle at various ZTs (n = 4 mice per genotype and time point). Representative data (A and B) from two independent experiments are shown as mean ± S.E.M. Two-tailed Student's t-tests were used for statistical analyses. **P*<0.05; ***P*<0.01 comparison between *Arntl*$^{LoxP/LoxP}$ and *Arntl*$^{LoxP/LoxP}$*Lyz2*^{Cre} at each time point.

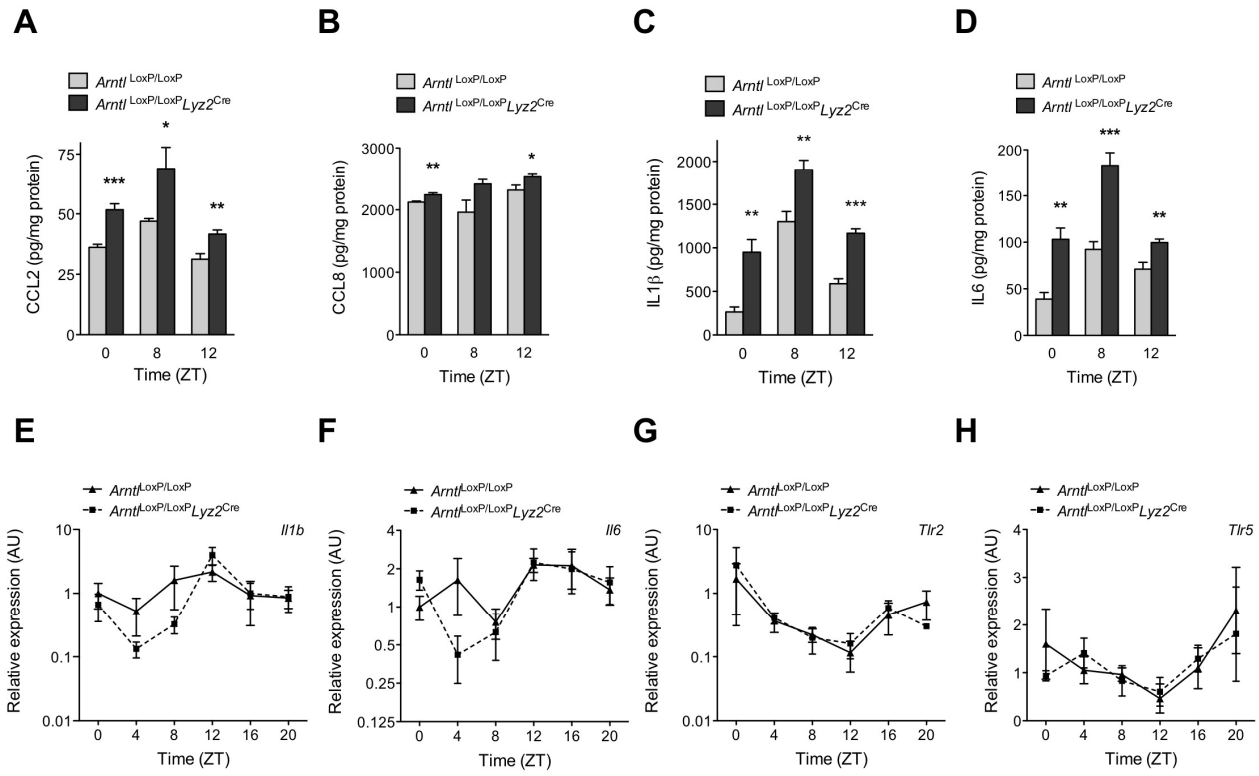

fig. S9. Characteristics of acute inflammation in *Arntl*$^{LoxP/LoxP}$*Lyz2*^{Cre} mice. (**A** to **D**) Concentration of CCL2 (A), CCL8 (B), IL1β (C), and IL6 (D) in the peritoneal fluid of *Arntl*$^{LoxP/LoxP}$ and *Arntl*$^{LoxP/LoxP}$*Lyz2*^{Cre} mice kept on a 12 hour light-dark cycle 2 hours after elicitation with thioglycollate at ZT0, ZT8, and ZT12 (n = 5 mice per genotype and time point). (**E-H**) Quantitative PCR analysis of *Il1b* (E), *Il6* (F), *Tlr2* (G), and *Tlr5* (H) mRNAs in blood monocytes of *Arntl*$^{LoxP/LoxP}$ and *Arntl*$^{LoxP/LoxP}$*Lyz2*^{Cre} mice kept on a 12 hour light-dark cycle at the various ZTs (n = 3-4 samples per genotype and time point). Pooled data from two independent experiments are shown as mean ± S.E.M and statistically analyzed by two-tailed Student's *t*-tests. **P*<0.05; ***P*<0.01; ****P*<0.001.

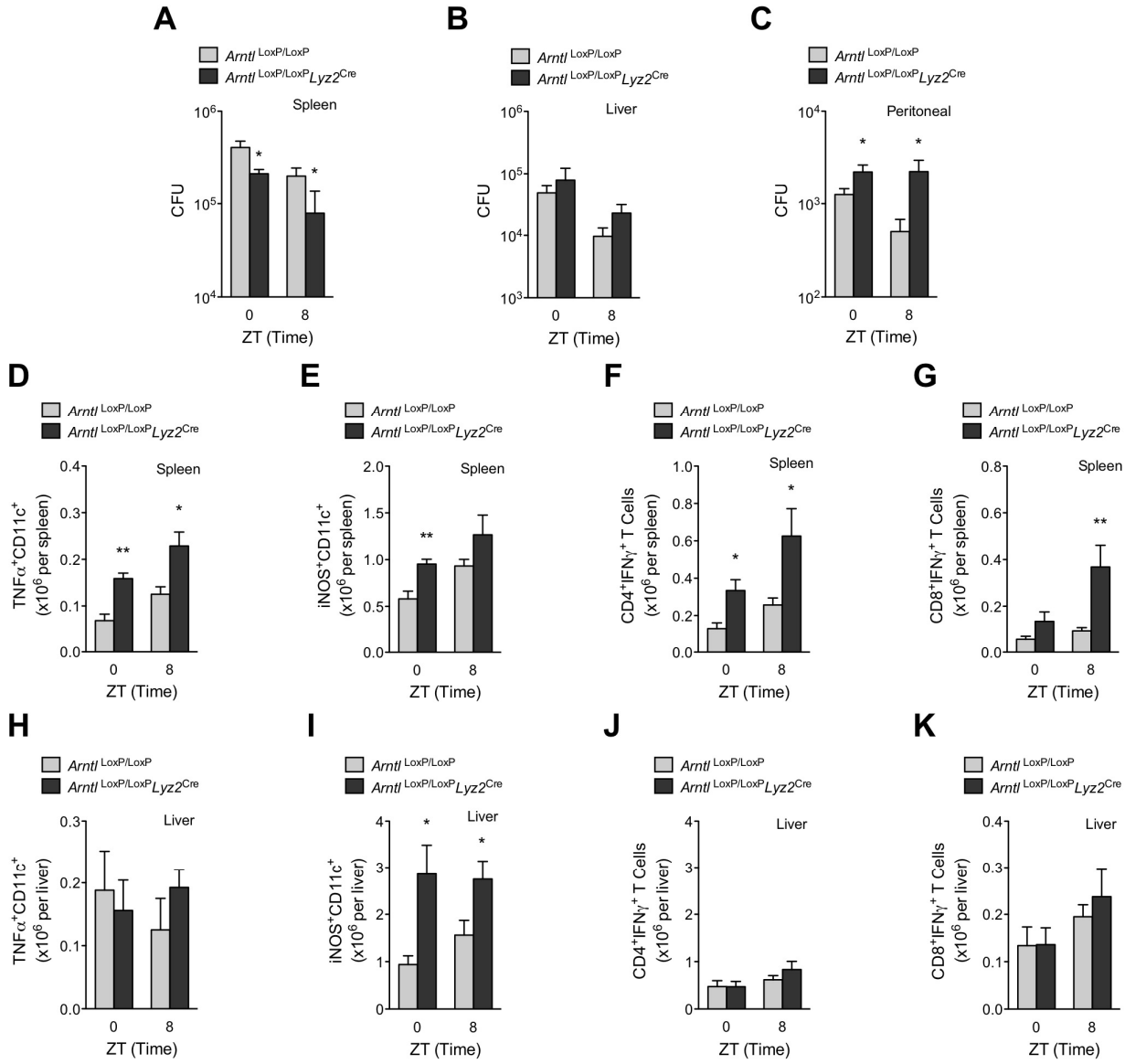

fig. S10. Quantification of bacterial burden and cytokine producing cells in *Arntl*$^{LoxP/LoxP}$ and *Arntl*$^{LoxP/LoxP}$*Lyz2*^{Cre} mice infected with *L. monocytogenes*. (**A** to **C**) *Arntl*$^{LoxP/LoxP}$ and *Arntl*$^{LoxP/LoxP}$*Lyz2*^{Cre} mice kept on a 12 hour light-dark cycle were intraperitoneally inoculated with 1x10^6 *L. monocytogenes* at ZT0 and ZT8, and colony

forming units (CFUs) recovered from the spleen (A), liver (B), and peritoneal cavity (C) were quantified 2 dpi (n = 4-6 mice per genotype and time point). (**D** to **K**) Numbers of $TNF\alpha^{+}CD11c^{+}$ (D and H), $iNOS^{+}CD11c^{+}$ (E and I), $IFN\gamma^{+}$ $CD4^{+}$ (F and J), and $CD8^{+}$ T (G and K) cells in spleens and livers, respectively, of $Arntl^{LoxP/LoxP}$ and $Arntl^{LoxP/LoxP}Lyz2^{Cre}$ mice kept on a 12 hour light-dark cycle 2 dpi with $1x10^{6}$ *L. monocytogenes* at ZT0 and ZT8 (n = 4-6 mice per genotype and time point). All data are presented as mean ± S.E.M and statistically analyzed by two-tailed Student's *t*-tests. $*P<0.05$; $**P<0.01$; $***P<0.001$.

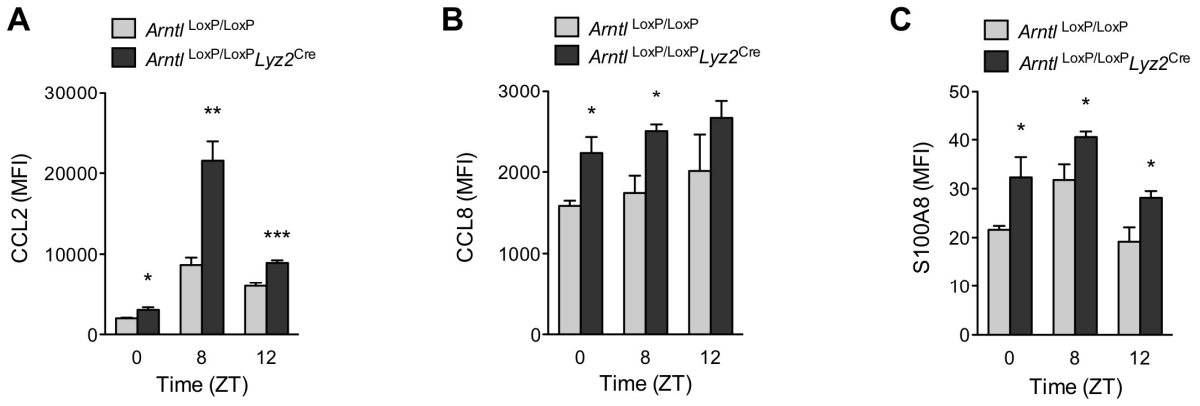

fig. S11. Chemokine expression in thioglycollate-elicited peritoneal monocytes. (**A** to **C**) Intracellular staining for CCL2 (A), CCL8 (B), and S100A8 (C) in peritoneal monocytes of *Arntl*$^{\text{LoxP/LoxP}}$ and *Arntl*$^{\text{LoxP/LoxP}}$*Lyz2*$^{\text{Cre}}$ mice kept on a 12 hour light-dark cycle 30 mins after injection of thioglycollate at various ZTs (n = 4-5 mice per genotype and time point). Representative data of two independent experiments are shown as mean ± S.E.M and analyzed using two-tailed Student's *t*-test. **P*<0.05; ***P*<0.01; ****P*<0.001.

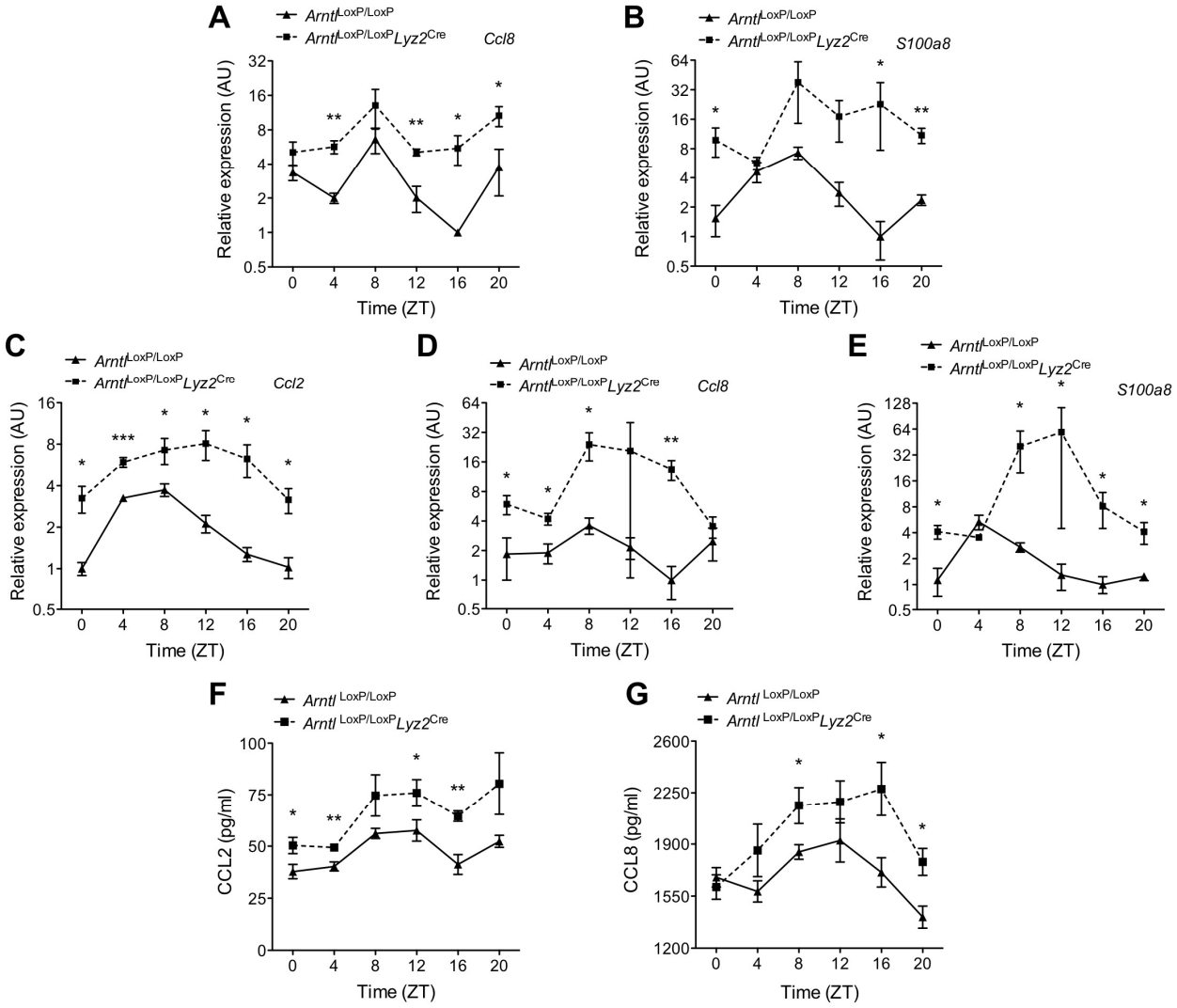

fig. S12. Chemokine expression in monocytes and macrophages of *Arntl*$^{LoxP/LoxP}$ and *Arntl*$^{LoxP/LoxP}$*Lyz2*^{Cre} mice. (**A** and **B**) Quantitative RT-PCR analysis for *Ccl8* (A) and *S100a8* (B) mRNA expression in blood monocytes of *Arntl*$^{LoxP/LoxP}$ and *Arntl*$^{LoxP/LoxP}$*Lyz2*^{Cre} mice during a 12 hour light-dark cycle (n = 3-4 samples per genotype and time point). (**C** to **E**) Quantitative RT-PCR analysis for *Ccl2* (C), *Ccl8* (D), and

S100a8 (E) mRNA expression in peritoneal macrophages of *Arntl*$^{LoxP/LoxP}$ and *Arntl*$^{LoxP/LoxP}$*Lyz2*^{Cre} mice during a 12 hour light-dark cycle (n = 4-5 mice per genotype and time point). (**F** and **G**) Serum CCL2 (F) and CCL8 (G) concentrations in *Arntl*$^{LoxP/LoxP}$ and *Arntl*$^{LoxP/LoxP}$*Lyz2*^{Cre} mice during a 12 hour light-dark cycle (n = 4-19 mice per genotype and timepoint). Pooled data from two to four independent experiments are presented as mean ± S.E.M and statistically analyzed with two-tailed Student's *t*-test. **P*<0.05; ***P*<0.01; ****P*<0.001.

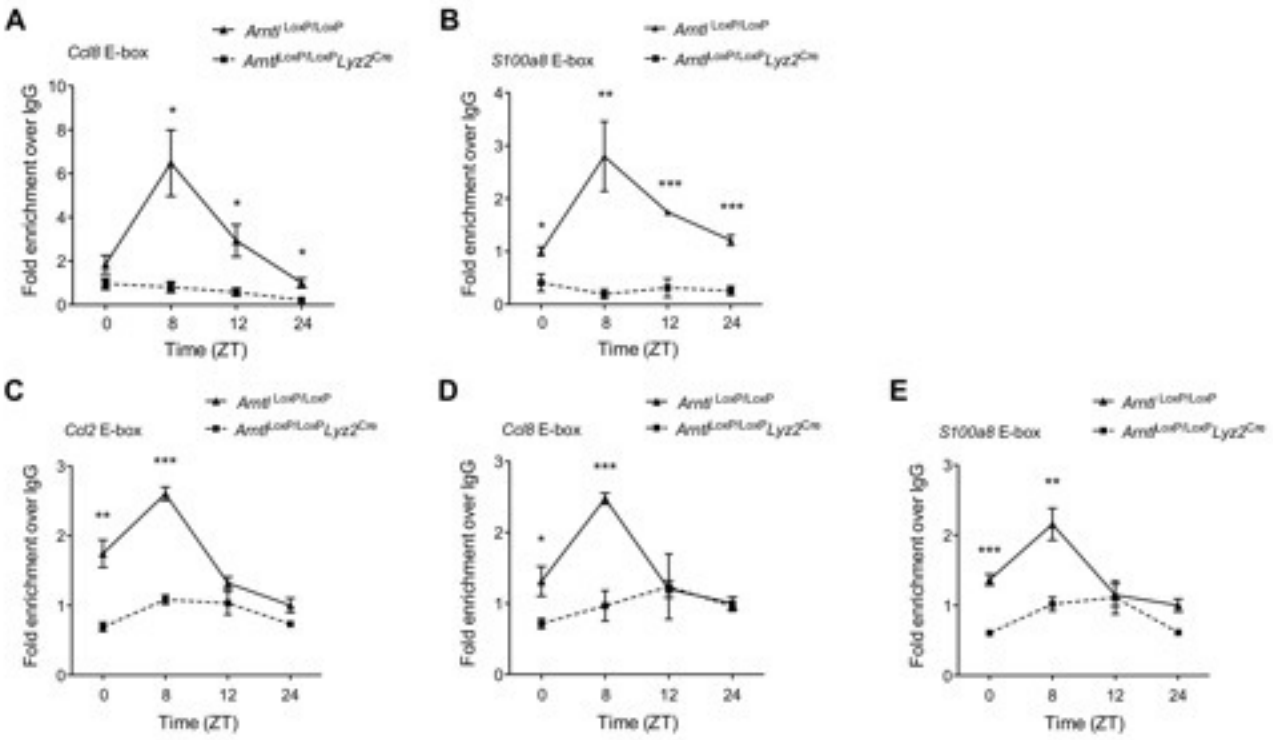

fig. S13. Circadian recruitment of BMAL1 and CLOCK to the chemokine promoters. (**A** and **B**) ChIP analysis of BMAL1 binding to the E-boxes in *Ccl8* (A) and *S100a8* (B) promoters (n = 4 samples per genotype and time point). (**C** to **E**) ChIP analysis of CLOCK binding to the E-boxes in promoters of *Ccl2* (C), *Ccl8* (D), and *S100a8* (E) genes (n = 4 samples per genotype and time point). Pooled data from two independent experiments are presented as mean ± S.E.M and statistically analyzed using two-tailed Student's *t*-test. **P*<0.05; ***P*<0.01; ****P*<0.001.

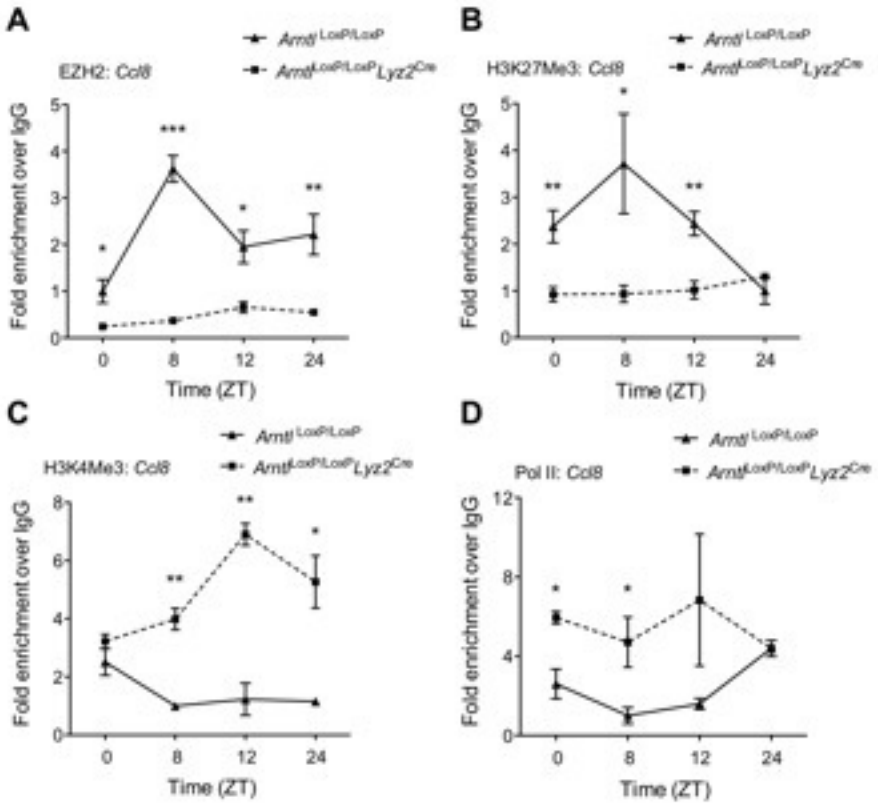

fig. S14. Circadian recruitment of PRC2 to the promoter of *Ccl8 gene*. (**A** to **D**) ChIP analysis for the recruitment of EZH2 (A) and Pol II (D) to the proximal promoter of the *Ccl8* gene (n = 4 samples per genotype and time point), and for H3K27Me3 (B) and H3K4Me3 (C) at the proximal promoter of *Ccl8* gene (n = 4 samples per genotype and time point). Pooled data from two independent experiments are presented as mean ± S.E.M and statistically analyzed using two-tailed Student's *t*-test. **P*<0.05; ***P*<0.01; ****P*<0.001.

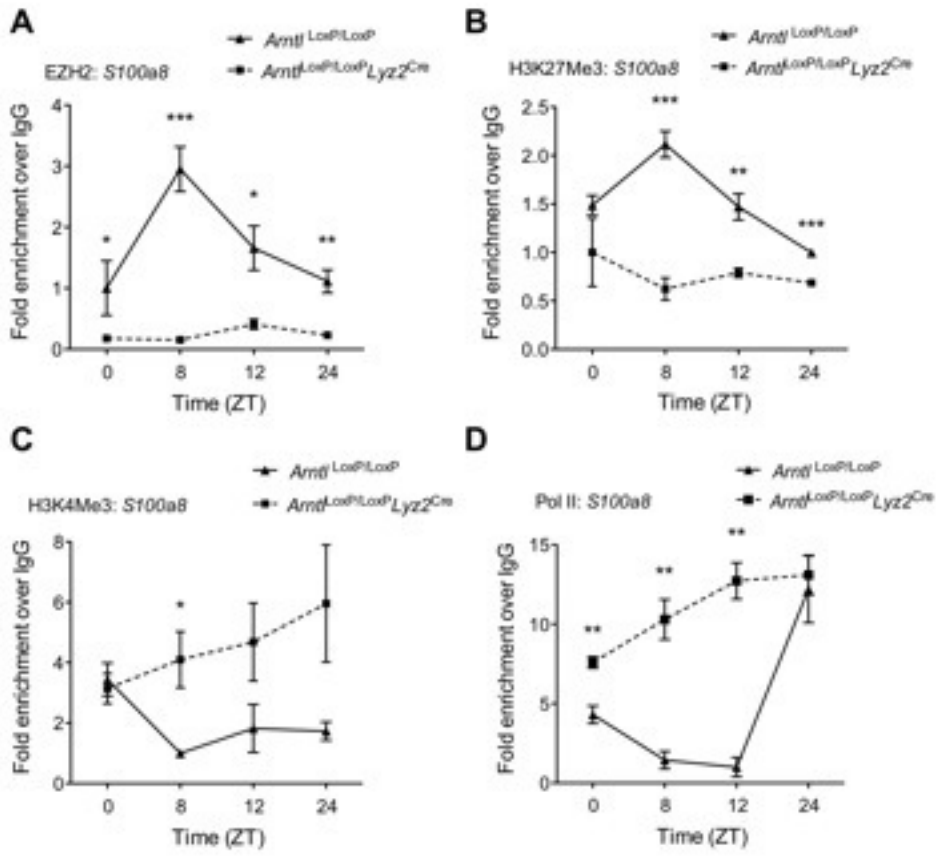

fig. S15. Circadian recruitment of PRC2 to the promoter of *S100a8 gene*. (**A** to **D**) ChIP analysis for the recruitment of EZH2 (A) and Pol II (D) to the proximal promoter of the *S100a8* gene (n = 4 samples per genotype and time point), and for H3K27Me3 (B) and H3K4Me3 (C) at the proximal promoter of *S100a8* gene (n = 4 samples per genotype and time point). Pooled data from two independent experiments are presented as mean ± S.E.M and statistically analyzed using two-tailed Student's *t*-test. **P*<0.05; ***P*<0.01; ****P*<0.001.

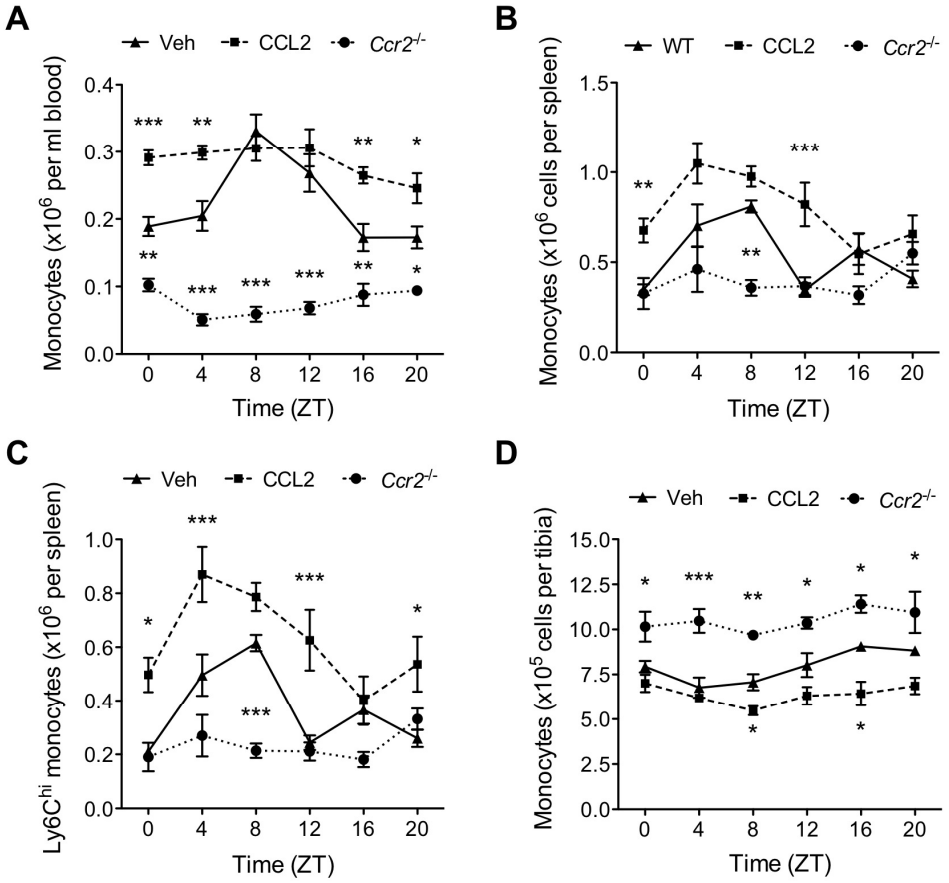

fig. S16. CCL2-CCR2 axis regulates diurnal variation in trafficking of monocytes. (**A** and **B**) Monocyte numbers in the blood (A) or spleens (B) of wild type or *Ccr2*$^{-/-}$ mice during a 12 hour light-dark cycle. Wild type mice kept on a 12 hour light-dark cycle were administered PBS (Veh) or CCL2 (20 μgkg^{-1}) 24 hours prior to quantification of monocytes (n = 4-5 mice per genotype/treatment and time point). (**C**) Ly6C^{hi} monocyte numbers in spleens of various groups during a 12 hour light-dark cycle (n = 4-5 mice per

genotype/treatment and time point). (**D**) Monocyte numbers in bone marrow of various groups during a 12 hour light-dark cycle (n = 4-5 mice per genotype/treatment and time point). All data are presented as mean ± S.E.M and statistically analyzed using two-way ANOVA. **P*<0.05; ***P*<0.01; ****P*<0.001 represent comparison between wild type Veh treated vs. CCL2 or *Ccr2*$^{-/-}$ at each time point.

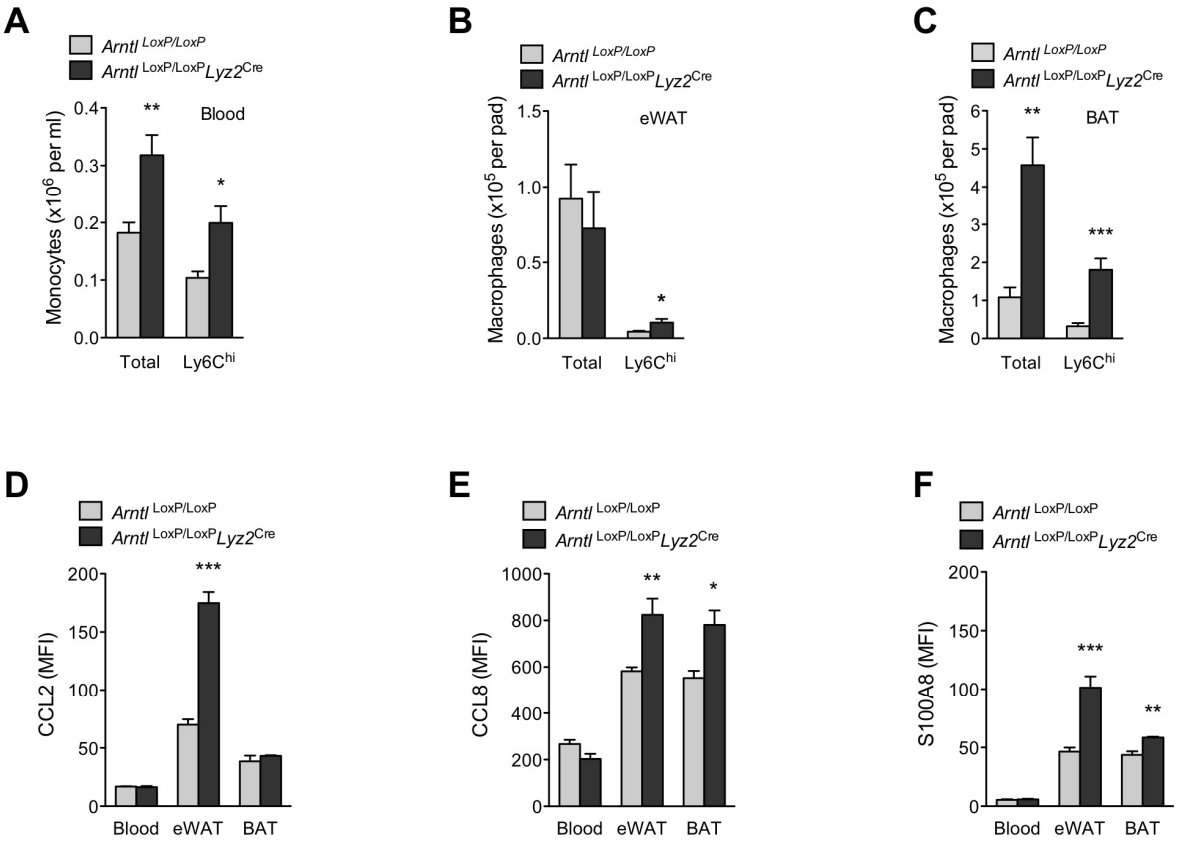

fig. S17. BMAL1 regulates monocyte trafficking during HFD feeding. *Arntl*$^{LoxP/LoxP}$ and *Arntl*$^{LoxP/LoxP}$*Lyz2*^{Cre} mice kept on a 12 hour light-dark cycle were housed at 30°C and fed HFD for 1 week. (**A** to **C**) Numbers of monocytes in blood (A), macrophages in eWAT (B), and macrophages in BAT (C) of *Arntl*$^{LoxP/LoxP}$ and *Arntl*$^{LoxP/LoxP}$*Lyz2*^{Cre} mice (n = 5 mice per genotype). (**D** to **F**) Expression of CCL2 (D), CCL8 (E), and S100A8 (F) in Ly6C^{hi} blood monocytes and adipose tissue macrophages of *Arntl*$^{LoxP/LoxP}$ and *Arntl*$^{LoxP/LoxP}$*Lyz2*^{Cre} mice (n = 5 mice per genotype). Representative data (A to C) from two independent experiments are shown as mean ± S.E.M and statistically analyzed using two-tailed Student's *t*-test. **P*<0.05; ***P*<0.01; ****P*<0.001.

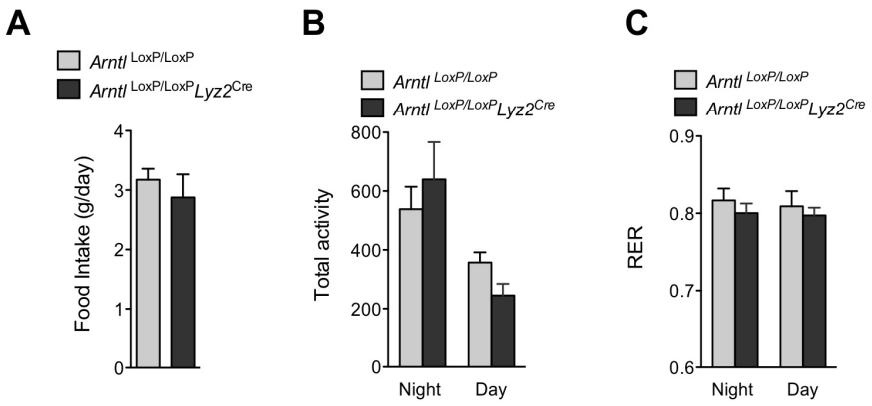

fig. S18. Behavioral characteristics of *Arntl*$^{LoxP/LoxP}$ and *Arntl*$^{LoxP/LoxP}$*Lyz2*^{Cre} mice on HFD. (**A** to **C**) Food intake (A), total activity (B), and RER (C) of obese *Arntl*$^{LoxP/LoxP}$ and *Arntl*$^{LoxP/LoxP}$*Lyz2*^{Cre} mice kept on a 12 hour light-dark cycle fed HFD (n = 4 mice per genotype). Data are presented as mean ± S.E.M and statistically analyzed using two-tailed Student's *t*-test.

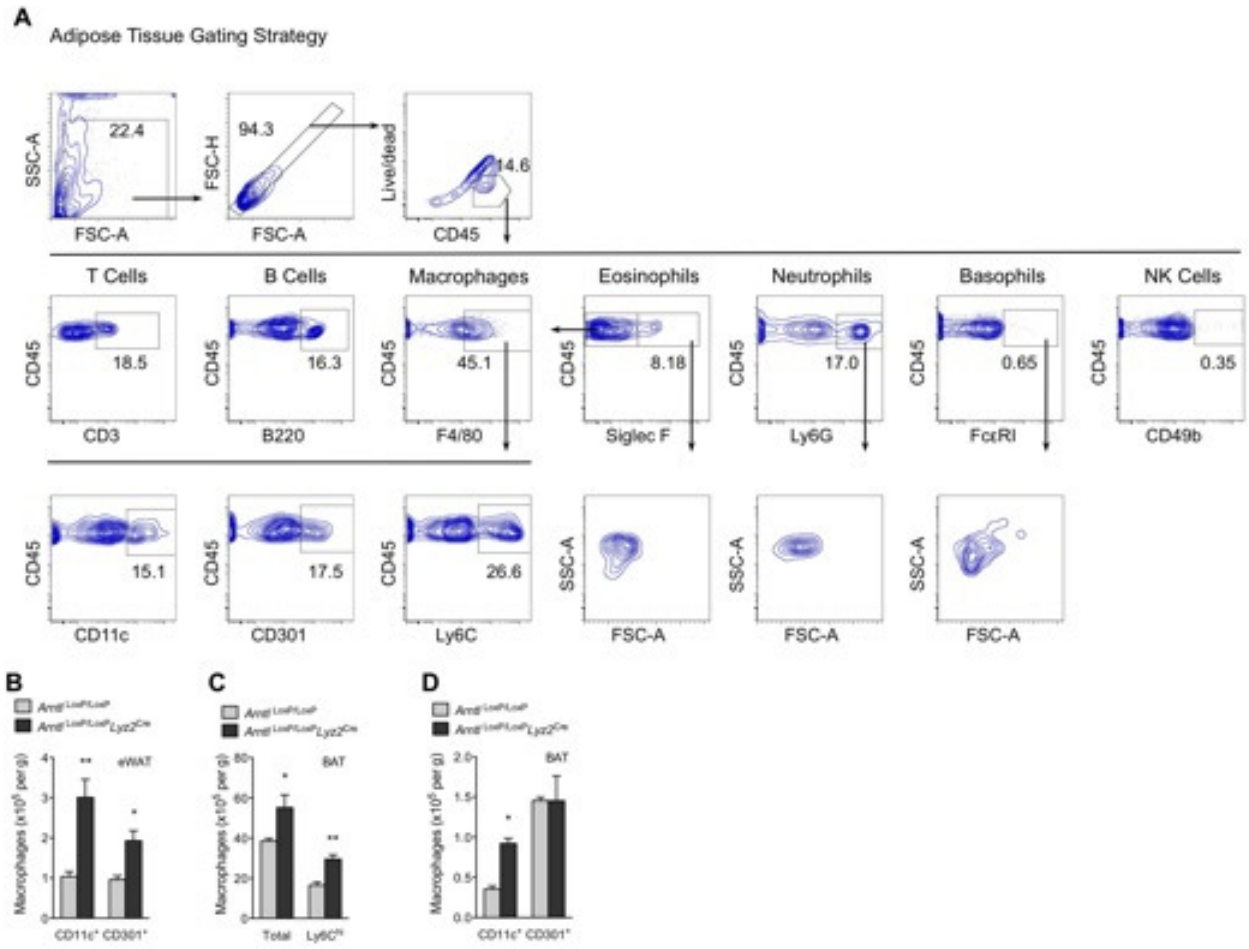

fig. S19. Gating strategy for analysis of immune subsets in adipose tissue. (**A**) Mononuclear cells were gated for forward and side-scatter (FSC/SSC), doublets, and live/dead prior to analysis of $CD3^+$ T cells, $B220^+$ B cells, Siglec $F^-F4/80^+$ macrophages, Siglec F^+ eosinophils, $Ly6G^+$ neutrophils, $Fc\varepsilon RI^+$ basophils/mast cells, and $CD49b^+$ NK cells. Macrophages subsets were identified as being $Ly6C^{hi}$, $CD301^+$, or $CD11c^+$. (**B** to **D**) Macrophage content and subtypes in eWAT (B) and BAT (C and D) of *Arntl*$^{LoxP/LoxP}$ and *Arntl*$^{LoxP/LoxP}$*Lyz2*^{Cre} mice fed high fat diet (n = 5 mice per genotype). Representative data (B to D) from two independent experiments are shown as mean ± S.E.M and statistically analyzed using two-tailed Student's *t*-tests. **P*<0.05; ***P*<0.01.

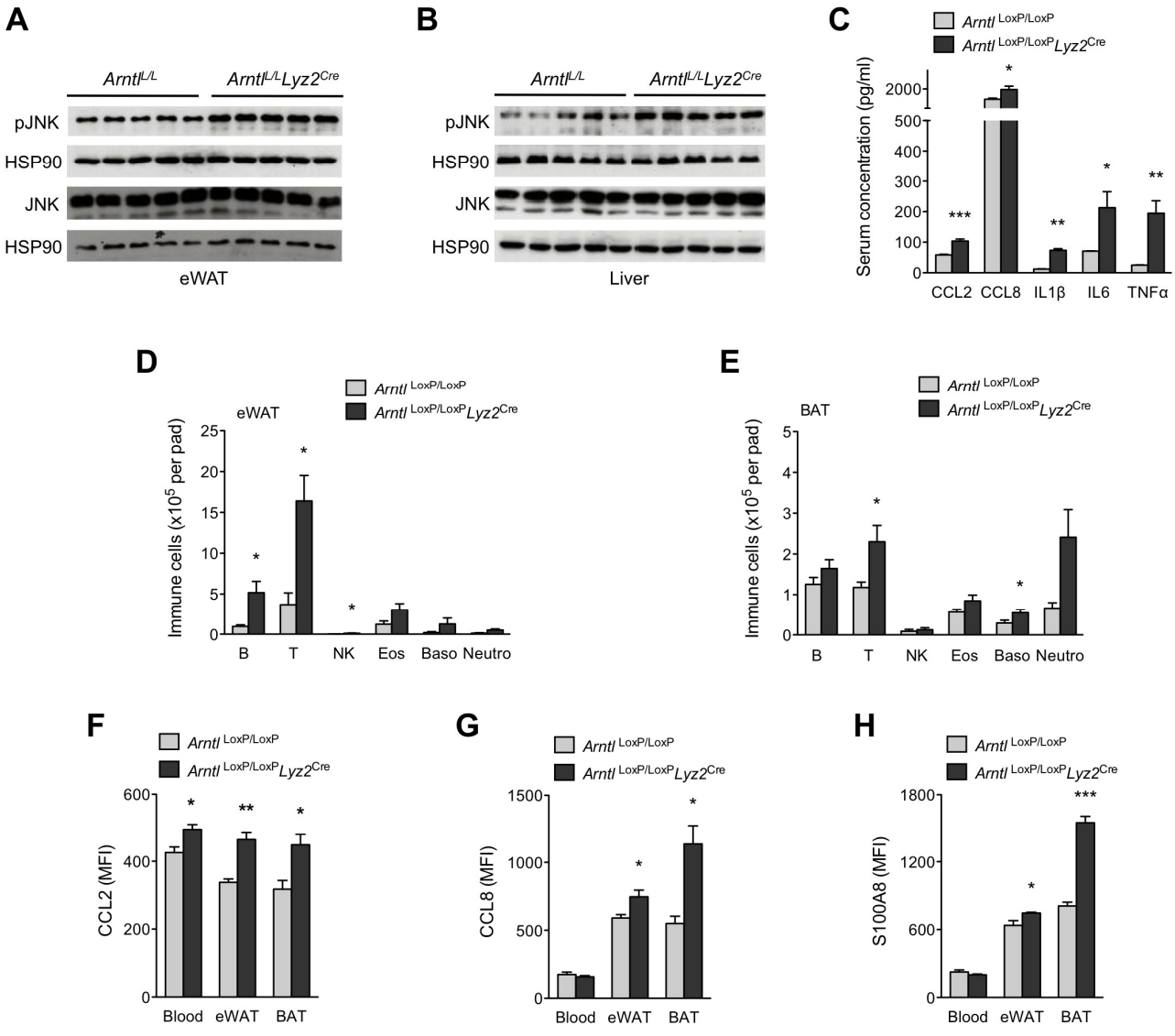

fig. S20. Evaluation of tissue inflammation in obese *Arntl*$^{\text{LoxP/LoxP}}$ and *Arntl*$^{\text{LoxP/LoxP}}$*Lyz2*$^{\text{Cre}}$ mice. (**A** and **B**) Immunoblots of total and phosphorylated JNK (pJNK) in eWAT (A) and livers (B) of obese *Arntl*$^{\text{LoxP/LoxP}}$ and *Arntl*$^{\text{LoxP/LoxP}}$*Lyz2*$^{\text{Cre}}$ mice fed HFD for 19 weeks and kept on a 12 hour light-dark cycle. (**C**) Serum concentration of chemokines and cytokines of obese *Arntl*$^{\text{LoxP/LoxP}}$ and *Arntl*$^{\text{LoxP/LoxP}}$*Lyz2*$^{\text{Cre}}$ mice (n = 4-5

mice per genotype). (**D** and **E**) Immune cell repertoire of eWAT (D) and BAT (E) of obese *Arntl*$^{LoxP/LoxP}$ and *Arntl*$^{LoxP/LoxP}$*Lyz2*^{Cre} mice (n = 4-5 mice per genotype). (**F** to **H**) Expression of CCL2 (F), CCL8 (G), and S100A8 (H) in blood monocytes and adipose tissue macrophages of obese *Arntl*$^{LoxP/LoxP}$ and *Arntl*$^{LoxP/LoxP}$*Lyz2*^{Cre} mice (n = 4-5 mice per genotype). Pooled data (A to C) or representative (D and E) of two independent experiments are shown as mean ± S.E.M and statistically analyzed using two-tailed Student's *t*-test. **P*<0.05; ***P*<0.01; ****P*<0.001.

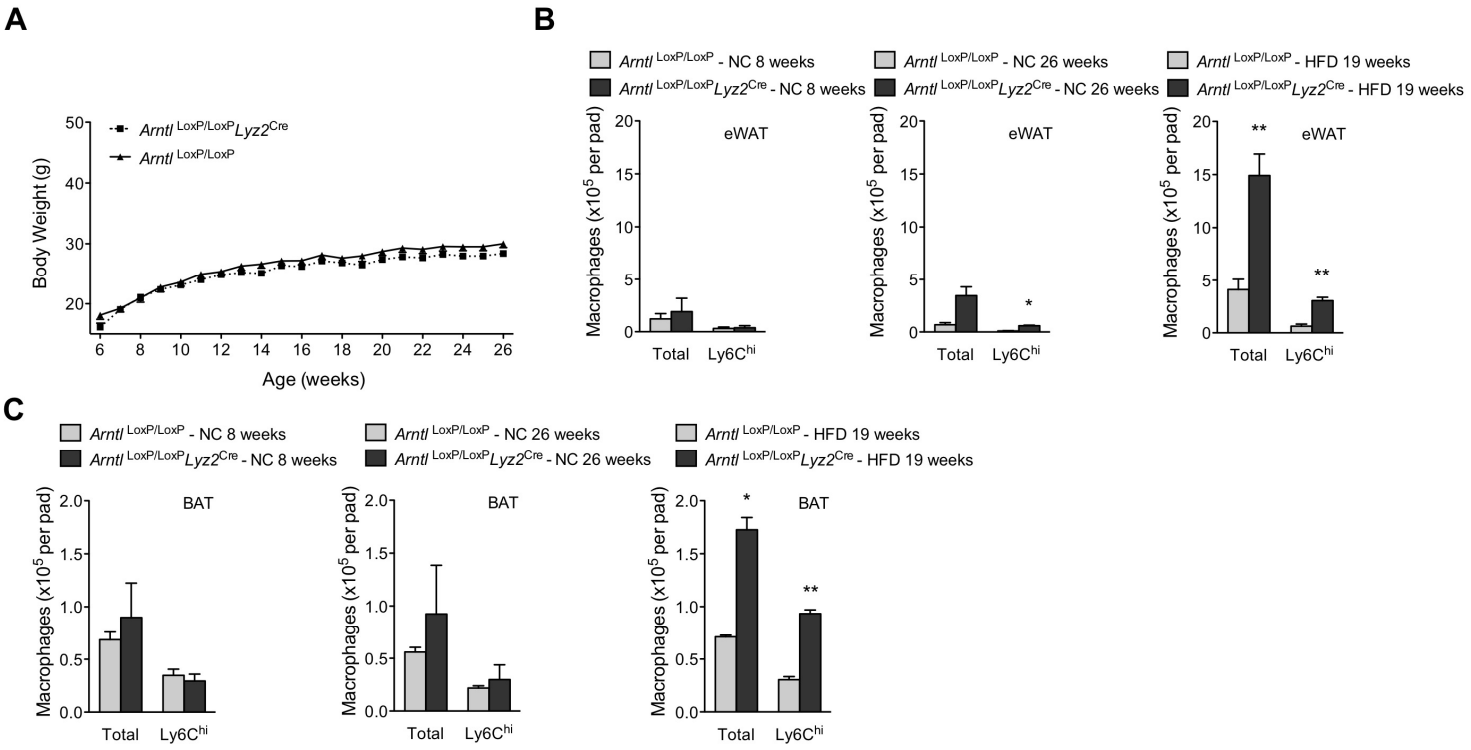

fig. S21. Characteristics of *Arntl*$^{LoxP/LoxP}$ and *Arntl*$^{LoxP/LoxP}$*Lyz2*^{Cre} mice on normal chow diet. (**A**) Body weight of *Arntl*$^{LoxP/LoxP}$ and *Arntl*$^{LoxP/LoxP}$*Lyz2*^{Cre} mice kept on a 12 hour light-dark cycle fed normal chow diet (NC) for 26 weeks (n = 4-5 mice per genotype). (**B** and **C**) Total and Ly6C^{hi} macrophage content in eWAT (B) and BAT (C) of Arntl$^{LoxP/LoxP}$ and Arntl$^{LoxP/LoxP}$Lyz2^{Cre} mice on various diets (n=3-5 mice per genotype). Representative data of two independent experiments are shown as mean ± S.E.M and statistically analyzed using two-tailed Student's *t*-test. **P*<0.05; ***P*<0.01.

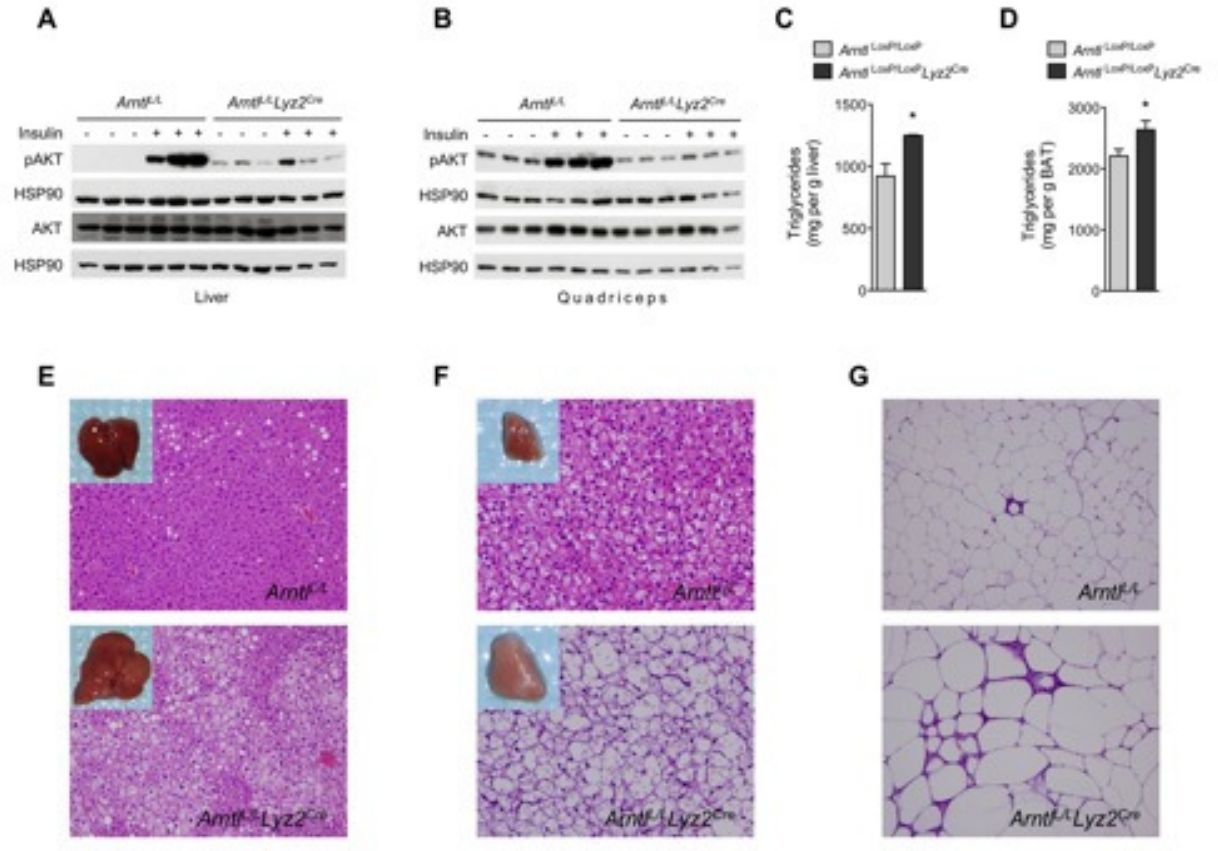

fig. S22. Metabolic characteristics of *Arntl*$^{LoxP/LoxP}$ and *Arntl*$^{LoxP/LoxP}$*Lyz2*^{Cre} mice on HFD. (**A** and **B**) Immunoblots of total and phosphorylated AKT (pAKT) in liver (A) and quadriceps (B) of obese *Arntl*$^{LoxP/LoxP}$ and *Arntl*$^{LoxP/LoxP}$*Lyz2*^{Cre} administered intraportal insulin. (**C** and **D**) Liver (C) and BAT (D) triglyceride content of obese *Arntl*$^{LoxP/LoxP}$ and *Arntl*$^{LoxP/LoxP}$*Lyz2*^{Cre} mice (n = 5 mice per genotype). (**E** to **G**) Representative sections of liver (E), BAT (F), and eWAT (G) of obese *Arntl*$^{LoxP/LoxP}$ and *Arntl*$^{LoxP/LoxP}$*Lyz2*^{Cre} mice stained with hematoxylin and eosin (H&E). Pooled data (A to D) and representative of two independent experiments (E to G) are shown as mean ± S.E.M and statistically analyzed using two-tailed Student's *t*-tests. **P*<0.05.

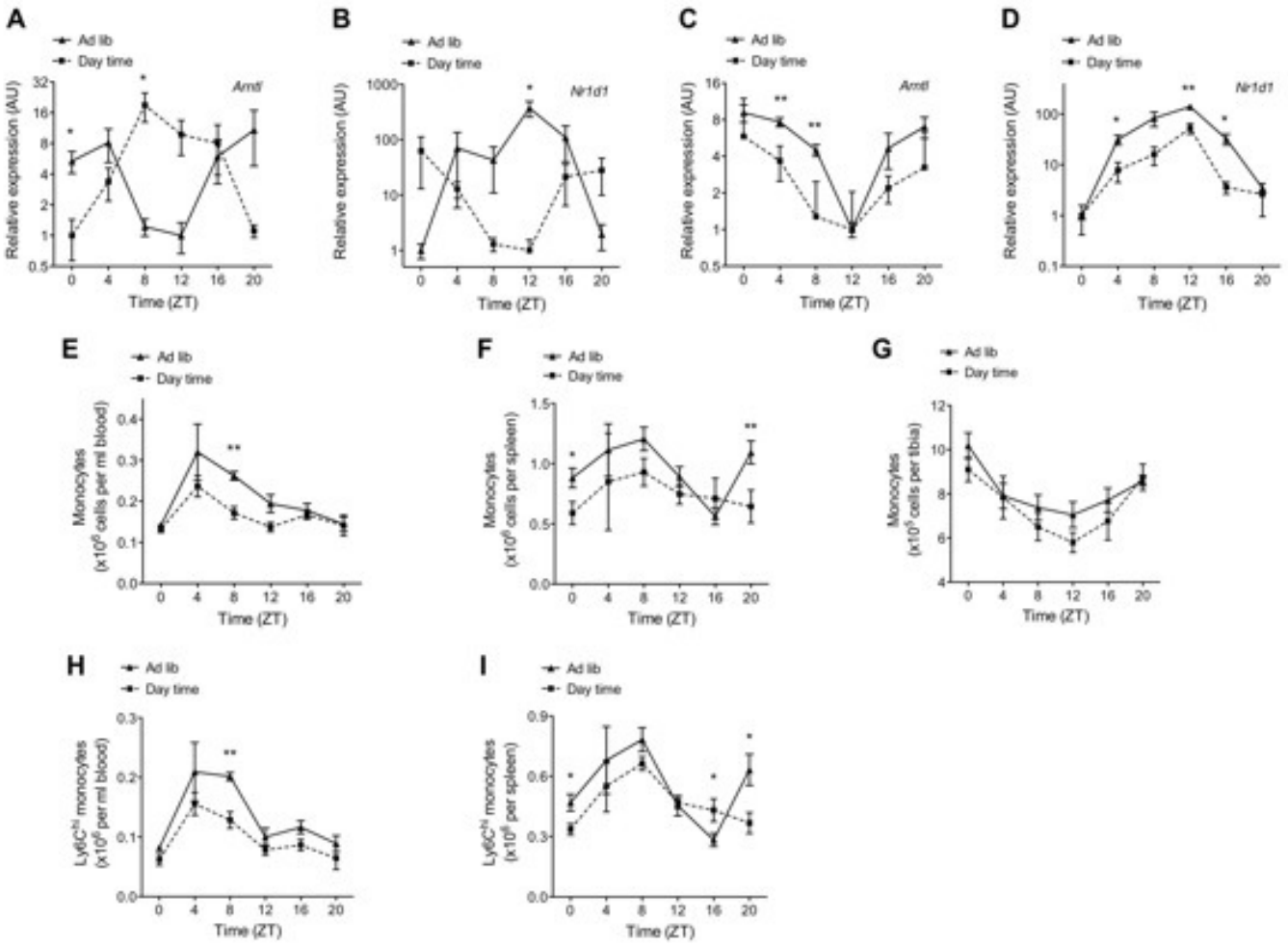

fig. S23. Time restricted feeding does not entrain the diurnal rhythms of monocytes. (**A** to **D**) Quantitative RT-PCR analysis of *Arntl* and *Nr1d1* mRNAs in liver (A and B) and peritoneal macrophages (C and D) of C57BL/6J mice fed *ad libitium* or exclusively during the light phase of a 12 hour light-dark cycle (n = 4-5 mice per treatment and time point). (**E** to **G**) Numbers of total monocytes in blood (E), spleen (F), and bone marrow (G) of C57BL/6J mice fed *ad libitium* or exclusively during the light phase of a 12 hour light-dark cycle (n = 4-5 mice per treatment and time point). (**H** and **I**) Numbers of Ly6C^{hi} monocytes in blood (H) and spleen (I) of C57BL/6J mice fed *ad libitium* or exclusively during the light phase of a 12 hour light-dark cycle (n = 4-5 mice per

treatment and time point). In E to I, rhythms of time-restricted animals are overlayed on data presented in Fig. 1 and fig. S3. All data are presented as mean ± S.E.M and statistically analyzed using two-tailed Student's *t*-test. **P*<0.05; ***P*<0.01.

table S1. Primers for chemokine E-boxes

Ccl2 forward	5'-CAGATTCTCCGGCCCATGA-3'
Ccl2 reverse	5'-CAGGTCAGAGGCAGAGTAGGATAAG-3'
Ccl8 forward	5'-AACCTCTCTTTACTCCATGGTAACC-3'
Ccl8 reverse	5'-TCCCACTGGATCAGGGATTCT-3'
S100a8 forward	5'-GCAGCAACAGCAATGAAATG-3'
S100a8 reverse	5'-AGCCATGTTCTCCAGGTGTC-3'

table S2. Primers for proximal promoter region of chemokines.

Ccl2 forward	5'-CGAGGGCTCTGCACTTACTC-3'
Ccl2 reverse	5'-AGGAGTAGCATCACCCTGGA-3'
Ccl8 forward	5'-ATTCTTGCTGAGCTGCCTTC-3'
Ccl8 reverse	5'-TTGTGCCTAATGGGAAATGA-3'
S100a8 forward	5'-TCCAACACTCCCACTTCCTC-3'
S100a8 reverse	5'-GGCTATGGAGACAACGCTCT-3'

table S3. Primers for core clock genes and chemokines.

Arntl forward	5'-AGAGGCGTCGGGACAAAATGAACAG-3'
Arntl reverse	5'-AACAGCCATCCTTAGCACGGTGA-3'
Nr1d1 forward	5'-CTTCATCCTCCTCCTCCTTCTA-3'
Nr1d1 reverse	5'-GTAATGTTGCTTGTGCCCTTG-3'
Dbp forward	5'-GCATTCCAGGCCATGAGAC-3'
Dbp reverse	5'-GTTCTTGTACCTCCGGCTCCA-3'
Ccl2 forward	5'-CATCCACGTGTTGGCTCA-3'
Ccl2 reverse	5'-GATCATCTTGCTGGTGAATGAGT-3'
Ccl8 forward	5'-TTCTTTGCCTGCTGCTCATA-3'
Ccl8 reverse	5'-AGCAGGTGACTGGAGCCTTA-3'
S100a8 forward	5'-CCCGTCTTCAAGACATCGTTTG-3'
S100a8 reverse	5-'ATATCCAGGGACCCAGCCCTAG-3'
36b4 forward	5'-GAGACTGAGTACACCTTCCCAC-3'
36b4 reverse	5′-ATGCAGATGGATCAGCCAGG-3′